Channeling of D^+ and He^+ Ions in Gold Crystals*

C. J. ANDREEN† AND R. L. HINES
Northwestern University, Evanston, Illinois
(Received 3 June 1966)

The transmitted intensity of D^+ and He^+ ions through gold crystals in the forward direction is measured as a function of crystal orientation for energies near 15 keV. The gold crystals have a (100) orientation and are mounted in a goniometer which can tilt the foil normal up to 60° away from the incident beam direction and which can rotate the foil about its normal. The detector can be tilted relative to the beam direction up to a maximum angle of 58°. Pronounced peaks are found in the transmitted intensity at low-index directions. Both directional and planar channeling are present. The peak widths are successfully interpreted in terms of a channel-entrance peak width and a channel-exit peak width. Energy analysis shows that the energy of the transmitted ions also has peaks in the low-index directions. The experimental values for the energy loss of the randomly scattered part of the ion beam agree with the theoretical predictions.

INTRODUCTION

IN two recent papers we show that channeled intensities of low-energy D^+ ions in single-crystal face-centered cubic (fcc) gold[1] and body-centered cubic (bcc) α-ion films[2] are closely related to the crystal structure. For both lattice types we find enhanced transmission in directions corresponding to the five channels calculated by Robinson and Oen[3] to be the most open ones. Planar channels are also confirmed. In both structures they originated from the two widest separated types of planes.

In order to explain long "tails" observed in measured range distributions by Davies *et al.*,[4] Robinson and Oen, in their computer studies, let a computer trace the history of ions traveling in an ordered structure. Different types of interatomic potentials were used. In preliminary studies it was found that 1% of 10-keV Cu atoms, slowing down in Cu according to the Bohr potential, made very long flights, predominantly in the ⟨001⟩ direction. At the present time structural effects due to channeling have been observed in range measurements,[5] ion reflection and transmission measurements,[6] sputtering yields,[7–10] secondary electron yields,[11] conversion-electron measurements,[12] and in nuclear reaction rates.[13–15] Theoretical works on channeling have recently been published by Lindhard,[16] Erginsoy,[17] and Lehmann and Leibfried.[18] The ions are separated in two main groups according to the type of motion they experience during the passage of the film. Ions which are scattered in a random way experience *ungoverned* motion while channeled ions experience *governed* motion.[16] Governed motion is further divided into directional and planar channeling.

The purpose of this investigation is to study channeling of light ions in evaporated gold films at energies lower than previously reported. It will be shown that both directional and planar channels are present. The most striking evidence for channeling is that the transmitted intensity in the forward direction shows pronounced peaks at low-index directions when measured as a function of foil orientation. The angular widths of these peaks are investigated and compared to the geometrical relations between the experimental apparatus and the crystal channels.

A secondary effect of channeling is the anisotropy in the energy loss experienced by the penetrating ions.[19–23] Energy is lost by electron excitation and through displacement of atoms. We call these losses electronic and nuclear energy losses, respectively. The energy loss of the ions experiencing ungoverned motion is compared with calculated values of the stopping power dE/dx according to Nielsen[24] and Lindhard and Scharff.[25] The reduction in the energy loss of the

* Supported by the U. S. Atomic Energy Commission.
† Present address: Chalmers University of Technology, Gothenburg, Sweden.

[1] C. J. Andreen, R. L. Hines, W. Morris, and D. E. Weber, Phys. Letters **19**, 116 (1965).
[2] C. J. Andreen, E. F. Wassermann, and R. L. Hines, Phys. Rev. Letters **16**, 782 (1966).
[3] M. T. Robinson and O. S. Oen, Phys. Rev. **132**, 2385 (1963).
[4] J. A. Davies, J. D. McIntyre, and G. A. Sims, Can. J. Chem. **40**, 1605 (1962).
[5] B. Domeij, F. Brown, J. A. Davies, and E. V. Kornelsen, Phys. Rev. Letters **12**, 363 (1964).
[6] R. S. Nelson and M. W. Thompson, Phil. Mag. **8**, 1677 (1963).
[7] A. L. Southern, W. R. Willis, and M. T. Robinson, J. Appl. Phys. **34**, 153 (1962).
[8] O. Almén and G. Bruce, Nucl. Instr. Methods **11**, 257 (1961).
[9] A. F. Tulinov, V. S. Kulikauskas, and M. M. Malov, Phys. Letters **18**, 304 (1965).
[10] J. M. Fluit, P. K. Rol, and J. Kistemaker, J. Appl. Phys. **34**, 690 (1963).
[11] H. Zscheile, Phys. Status Solidi **11**, 159 (1965).
[12] G. Astner, I. Bergström, B. Domeij, L. Eriksson, and A. Persson, Phys. Letters **14**, 308 (1965).
[13] E. Bøgh, J. A. Davies, and K. O. Nielsen, Phys. Letters **12**, 129 (1964).
[14] M. W. Thompson, Phys. Rev. Letters **13**, 756 (1964).
[15] B. Domeij and K. Björkqvist, Phys. Letters **14**, 127 (1965).
[16] J. Lindhard, Kgl. Danske Videnskab. Selskab., Mat. Fys. Medd. **34**, No. 14 (1965).
[17] C. Erginsoy, Phys. Rev. Letters **15**, 360 (1965).
[18] C. Lehmann and G. Leibfried, J. Appl. Phys. **34**, 2821 (1963).
[19] C. Erginsoy, H. E. Wegner, and W. M. Gibson, Phys. Rev. Letters **13**, 530 (1964).
[20] A. R. Sattler and G. Dearnaley, Phys. Rev. Letters **15**, 59 (1965).
[21] W. M. Gibson, C. Erginsoy, H. E. Wegner, and B. R. Appleton, Phys. Rev. Letters **15**, 357 (1965).
[22] S. Datz, T. S. Noggle, and C. D. Moak, Phys. Rev. Letters **15**, 254 (1965).
[23] B. R. Appleton, C. Erginsoy, H. E. Wegner, and W. M. Gibson, Phys. Letters **19**, 185 (1965).
[24] *Electromagnetically Enriched Isotopes and Mass Spectroscopy*, edited by M. L. Smith (Academic Press Inc., New York, 1956), p. 68.
[25] J. Lindhard and M. Scharff, Phys. Rev. **124**, 128 (1961).

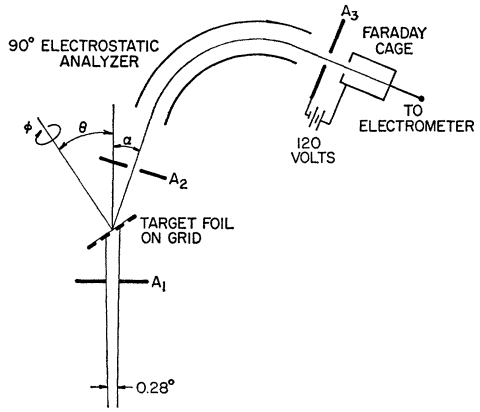

FIG. 1. Experimental arrangement for measuring the transmitted intensities of ions through a crystal as a function of the tilt angle θ and the rotation angle φ. The diameters of the apertures are A_1=0.75 mm, A_2=0.75 mm, and A_3=3 mm. The distance between the foil and aperture A_1 is 50 mm and the distance between the foil and aperture A_2 is 32 mm. The ranges of possible angles are $-60°\leq\theta\leq+60°$, $0°\leq\varphi\leq360°$, and $-3°\leq\alpha\leq+58°$. The distance between the analyzer plates is about 20 mm. The direction of the ion beam is fixed.

channeled ions is interpreted in terms of directional and planar channeling.

EXPERIMENTAL METHOD

Apparatus

The bombardment apparatus has been described earlier.[26] The goniometer, the energy analyzer, and the detector geometries used in this investigation are shown in Fig. 1. Details about the goniometer can be found elsewhere.[1] The angle subtended by the analyzer-detector system is here decreased to 1.4°. In addition the detector alone, or the analyzer-detector system as shown in Fig. 1, can be rotated an angle α about the same axis as the θ rotation. α can be varied from $-3°$ to $+58°$ relative to the beam direction. The beam is confined to a central area on the foil of about 1 mm in diameter. All measurements are done with the foil at room temperature. A copper cylinder in the vicinity of the crystal can be cooled down to liquid-nitrogen temperatures to reduce contamination of the gold target.

Foil Preparation

The gold single crystals are grown in a conventional vacuum system at 10^{-5} Torr by evaporating gold onto hot rocksalt substrates which are cleaved in air just prior to their insertion in the vacuum system. In order to grow continuous films of thicknesses down to 200 Å it is necessary to evaporate an intermediate single-crystal silver film. During the growth of the silver crystal, about 1000 Å thick, the substrate is held at about 150°C. Gold is then evaporated onto the silver at a temperature of about 200°C. The evaporation rates are about 1–5 Å/sec. The gold-silver film is floated on water and the silver is then disolved in 30% HNO_3. The gold crystal is carefully rinsed and picked up on a 75 mesh Cu grid 3 mm in diameter. After the foil has dried on the grid the surface is shiny and without any visible wrinkles. The film is then checked in an electron microscope. No holes are present in the films which have been used for measurements without the energy analyzer and all films had perfect single-crystal diffraction patterns. The epitaxial relations are $\{100\}_{NaCl}\|\{100\}_{Ag}$ and $\{100\}_{Ag}\|\{100\}_{Au}$. The crystals are self supporting down to an estimated thickness of 50Å. Further details about the growth of single-crystal silver and gold films can be found elsewhere.[27] The thickness of the gold crystals has been measured from the optical transmission. The transmission coefficient of a monochromatic light beam is known as a function of the thickness.[28] In addition, the stacking faults, extending diagonally through the foils, have been used to determine the thickness. Results obtained by the two methods do not differ by more than 5–10%.

Measuring Procedure

The azimuthal angle φ in Fig. 1 is an arbitrary angle which has to be related to a known low-index crystallographic direction. The $\langle011\rangle$ channels have been used for this purpose. They are the most open channels in a fcc lattice and are found by rotating φ, keeping θ constant at 45°. The presence of four strong peaks at $\theta=45°$ indicates that the film is a single crystal. When the orientation of the crystal relative to the goniometer is known, the intensity as a function of θ can be measured for different planes. The two planes (100) and (110) have been chosen here. The most important plane $\{111\}$ can be found for $|\theta|\geq35°$ and the transmitted intensity is then maximized by changing both φ and θ.

When the energy analyzer is put in between the goniometer and the detector, the most probable energy loss ΔE_{mp} is obtained as a function of θ by maximizing the transmitted intensity i for a set of values of θ in a particular plane. This is done by varying the voltage on the analyzer plates. For some of the θ values the intensity is also measured for values of φ corresponding to high-index planes. This intensity does not show any sharp peaks as a function of θ. The energy E of the incident beam is kept constant while ΔE_{mp} and i are obtained as functions of θ and φ. If the analyzer is not used, the detector is attached directly to the goniometer and integrates over all energies in a specific direction.

RESULTS

Transmitted Intensity and Energy Loss

The transmitted intensity i and the most probable energy loss ΔE_{mp} for 25-keV He^+ ions in a 275 Å-thick

[26] R. L. Hines and R. Arndt, Phys. Rev. 119, 623 (1960).

[27] D. W. Pashley, Phil. Mag. 4, 324 (1959).

[28] P. Rouard, D. Malé, and J. Trompette, J. Phys. Radium 14, 587 (1953).

gold film are shown in Fig. 2 as functions of θ in the planes (100) and (110) for $\alpha=0°$. The smooth symmetric curves (solid lines) show the randomly scattered part and the corresponding energy loss in high-index crystallographic planes. These curves reflect the behavior of a randomly oriented polycrystalline gold film as confirmed by measurements. Figure 3 shows the same functions $i(\theta)$ and $\Delta E_{mp}(\theta)$ for 23 keV D^+ ions in a 550-Å-thick gold crystal. In both Figs. 2 and 3 the governed motion in the (100) plane is divided into two parts, indicated by dashed lines. These two parts represent directional and planar channeling. As far as the intensity functions are concerned the separation is made in the way described below.

The minima in the total intensity close to $\theta=-40°$ correspond to a very high index direction. No directional channeling is expected at this point. The intensity therefore originates from planar channeling. The same arguments also hold for the minima at about $\theta=-5°$, although the channel peaks might not be completely resolved at this point. The dashed lines are drawn close to these minima in a way that closely resembles the profile of the random part. Peaks corresponding to the

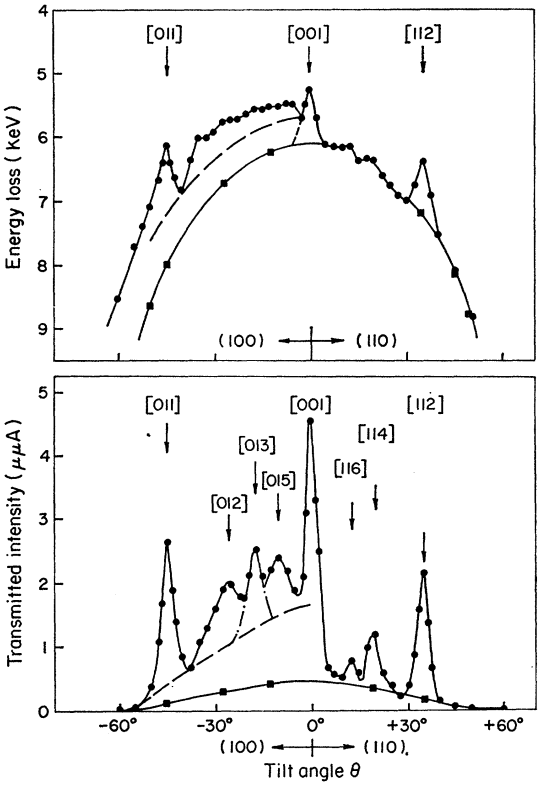

FIG. 2. Energy loss and transmitted intensity distributions for 25-keV He^+ ions transmitted through a 275-Å-thick single-crystal gold film. Arrows point at the angles for the indicated low-index directions in the two planes (100) and (110). Solid lines running through squares represent random quantities. Dashed lines represent dividing lines between directional and planar contributions. The dot dashed line indicates the line shape of channel [013]. Incident ion current is 1.9×10^{-9} A.

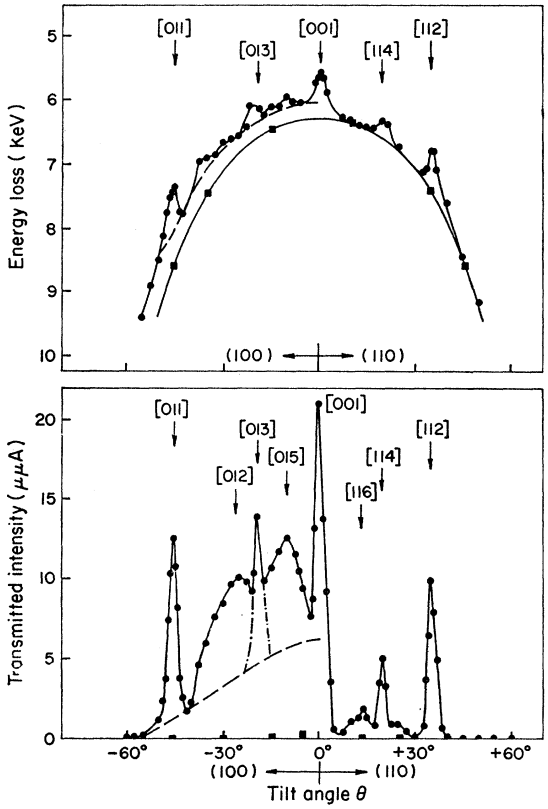

FIG. 3. Energy loss and transmitted intensity distributions for 23-keV D^+ ions transmitted through a 550-Å-thick single-crystal gold film. Arrows point at the angles for the indicated low-index directions in the two planes (100) and (110). Solid lines running through squares represent random quantities. Dashed lines represent dividing lines between directional and planar contributions. The dot-dashed line indicates the line shape of the channel [013]. Incident ion current is 1.1×10^{-9} A.

[012], [013], and [015] directions with a half-width at half-maximum of 2.5° (the same as for the other nicely resolved peaks) can now be superimposed on top of the planar part. The sum coincides nicely with the measured intensity.

The ratios of directional to planar channeling are expected to be much less dependent on the effective foil thickness than are the intensities themselves. If these ratios are compared within the (100) plane, the following expected order of importance amongst the peaks is obtained: ⟨011⟩, ⟨001⟩, ⟨013⟩, ⟨012⟩, and ⟨015⟩. This is found for both D^+ and He^+ ions. No planar channeling is found in the (110) plane. Despite the fact that a "cutoff" in planar channeling exists between {100} and {110} planes, peaks are present in the (110) plane corresponding to the [114] and [116] channels. The presence of the peaks [012], [013], [114], and [116] proves that the peaks can not be accounted for only by adding up planar contributions.

Figure 4 shows the transmitted intensity and the energy loss as functions of φ for $\theta=45°$ for 25-keV He^+ ions in the same foil as in Fig. 2. The curves are obtained

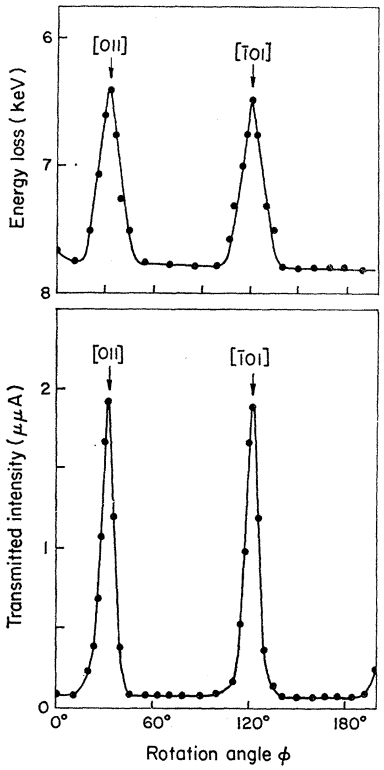

FIG. 4. Energy loss and transmitted intensity distributions for 25-keV He^+ ions transmitted through a 275 Å-thick single-crystal gold film tilted at an angle $\theta=45°$. Arrows point at the φ values for the indicated low-index directions. Incident ion current is 1.9×10^{-9} A. The curves are obtained after about 30 min of bombardment.

after the foil has been bombarded for about half an hour. It is seen that the (110) plane which would appear at $\varphi=76°$ and $\varphi=166°$ is completely absent.

Using 16-keV D^+ ions channeled through a 950-Å-thick gold crystal, it has been found that the relationship between planar contributions from $(\bar{1}\bar{1}1)$, (100), and (110) planes (separated from directional channeling as described above) at $|\theta|=35°$ is about

$$(110):(100):(\bar{1}\bar{1}1)=0:1:2.$$

This relation gives the experimental order of importance amongst the planes. A comparison between Figs. 2 and 3 reveals the following facts:

(a) The peak width is generally smaller for D^+ ions than for He^+ ions.

(b) The transmission of D^+ ions in the forward direction is higher despite the fact that D^+ ions pass through twice the thickness of gold.

(c) The same eight low-index directions are represented by peaks in the intensity functions at the expected angles and with approximately the same relative intensities.

(d) The intensity of ions experiencing ungoverned motion is relatively small for D^+ ions.

The effects of several low-index planes intersecting at a low-index direction are not known in detail at the present time. However, this problem is believed to be intimately related to the hard-sphere radius. For a small hard-sphere radius, the open area seen along a high-index direction in a low-index plane is a large fraction of the total area. In a direction where several low-index planes intersect, the additional open area is small. A calculation based on a radius of 0.04 a_g, where a_g is the lattice constant for gold, shows that the experimental order amongst the directions present in Figs. 2 and 3 does not change.

TABLE I. The peak widths σ_θ, σ_φ, and $\sigma_\theta/\sigma_\varphi$ are listed for four different channels. Different foils and energies are used. The agreement between $\sin\theta$ and $\sigma_\theta/\phi_\varphi$ is seen to be good.

hkl	θ (deg)	σ_θ (deg)	σ_φ (deg)	$\sigma_\theta/\sigma_\varphi$	$\sin\theta$
015	11.3	2.20	10.45	0.211	0.196
013	18.5	1.65	4.75	0.348	0.316
		2.30	6.50	0.354	
012	26.5	2.20	5.15	0.428	0.448
011	45.0	1.80	2.50	0.720	0.707
		2.00	2.80	0.715	
		2.60	3.80	0.686	
		2.30	3.16	0.724	

The peaks in the intensity curves are approximated by Gaussian curves. In particular, the relative transmitted intensity P_θ as a function of θ near a channel direction is given by the relation

$$P_\theta=\exp[-(\theta-\theta_0)^2/2\sigma_\theta^2] \quad \text{for} \quad \alpha=0,\ \varphi=\varphi_0, \quad (1)$$

where $(\theta_0;\ \varphi_0)$ is the angular position of a low-index direction and σ_θ is the characteristic half-width. P_θ is interpreted as the relative probability that an ion incident at a small angle $(\theta-\theta_0)$ to a channel will be channeled and detected within the small angular interval set by the detector.

The relative transmitted intensity P_φ as a function of φ close to a channel direction $(\theta_0;\ \varphi_0)$ is

$$P_\varphi=\exp[-(\varphi-\varphi_0)^2/2\sigma_\varphi^2] \quad \text{for} \quad \alpha=0,\ \theta=\theta_0, \quad (2)$$

where σ_φ is the characteristic half-width. In addition the relative probability $P_{1\theta}$ for an ion to be accepted into a channel $(\theta_0,\ \varphi_0)$ as a function of θ is denoted by

$$P_{1\theta}=\exp[-(\theta-\theta_0)^2/2\sigma_{1\theta}^2] \quad \text{for} \quad \alpha=\theta-\theta_0,\ \varphi=\varphi_0, \quad (3)$$

where $\sigma_{1\theta}$ is the characteristic half-width. The condition that $\alpha=\theta-\theta_0$ means that the detector is always kept aligned with the channel axis. The relative probability $P_{2\theta}$ for an ion to emerge from a channel at an angle α

TABLE II. The peak shift $\delta\theta$ is listed for three values of the detector position α_0. The ratio $\alpha_0/\delta\theta$ has an average value of 2.57. This value gives the ratio $\sigma_{1\theta}/\sigma_{2\theta}=0.8$ as compared with 0.74 obtained from direct measurements of $\sigma_{1\theta}$ and $\sigma_{2\theta}$.

α_0 (deg)	$\delta\theta$ (deg)	$\alpha_0/\delta\theta$
5.0	1.84±0.13	2.72±0.20
10.0	3.80±0.25	2.63±0.19
15.0	6.40±0.40	2.35±0.15

TABLE III. Calculated and measured values of the total stopping power dE/dx in gold for D^+ and He^+ ions in high-index directions. (N) refers to the theoretical expression for the nuclear energy loss given by Nielsen. (LS) refers to the electronic energy loss given by Lindhard and Scharff.

Ion	E (keV)	b/a	K	v/v_0	$(dE/dx)_n^{(N)}+(dE/dx)_{el}^{(LS)}$ (eV/Å)	expt. (eV/Å)
He^+	25	0.81	300	0.48	10.0	12±1
D^+	13	0.98	160	0.45	4.9	6±1
	23	0.74	260	0.64	7.0	8±1

with respect to the channel axis $(\theta_0; \varphi_0)$ is given by

$$P_{2\theta}=\exp[-\alpha^2/2\sigma_{2\theta}^2] \quad \text{for} \quad \theta=\theta_0,\ \varphi=\varphi_0, \qquad (4)$$

where $\sigma_{2\theta}$ is the characteristic half-width.

Measured values of σ_θ, $\sigma_{1\theta}$, and $\sigma_{2\theta}$ for ⟨011⟩ channels in a gold foil 660 Å±40 Å thick are $\sigma_\theta=2.7°\pm0.1°$, $\sigma_\theta=3.4°\pm0.1°$, and $\sigma_{2\theta}=4.6°\pm0.1°$. These values are for 9-keV D^+ ions. Measured values of σ_θ and σ_φ for several different channels are given in Table I. If the detector is set at an angle α_0, the peak position is found to be shifted from the channel direction by an amount $\delta\theta$. Table II gives values of α_0, $\delta\theta$ and their ratio for D^+ ions in the 660-Å gold crystal.

Experimental values for dE/dx have been obtained by plotting the total energy loss as a function of effective foil thickness d which varies as $1/\cos\theta$. A straight line is fitted to the experimental points. The results are presented in Table III.

The way of separating directional and planar channeling in the energy loss curves is based on the same arguments which were used above. However, for $\theta>50°$ the separation is somewhat arbitrary. No peaks are observed corresponding to the [012], [013], aud [015] directions. Table IV gives the percentage reduction in the energy loss in the [011], [001], and [112] directions which are the three most open crystallographic directions. No sign of the (110) plane is found in the energy distributions.

TABLE IV. The most probable energy losses for the random part $\Delta E_{mp}{}^r$ and the reduction in energy loss for the channeled parts $\Delta E_{mp}{}^r-\Delta E_{mp}$ for He^+ and D^+ ions in three directions in gold taken from Figs. 2 and 3. The bombarding particle energy is 25 keV for the He^+ ions and 23 keV for the D^+ ions. $(\Delta E_{mp}{}^r-\Delta E_{mp})/\Delta E_{mp}{}^r$ represents the percentage decrease in energy loss due to channeling.

Ion	hkl	θ (deg)	ΔE_{mp} (keV)	$\Delta E_{mp}{}^r$ (keV)	$\Delta E_{mp}{}^r-\Delta E_{mp}$ (keV)	$(\Delta E_{mp}{}^r-\Delta E_{mp})/\Delta E_{mp}{}^r$ (%)
He^+	011	−45	6.1	8.0	1.9	24±2
	001	0	5.2	6.1	0.9	15±2
	112	+35	6.4	7.2	0.8	11±1
D^+	011	−45	7.3	8.6	1.3	15±2
	001	0	5.6	6.3	0.7	11±1
	112	+35	6.8	7.5	0.7	9±1

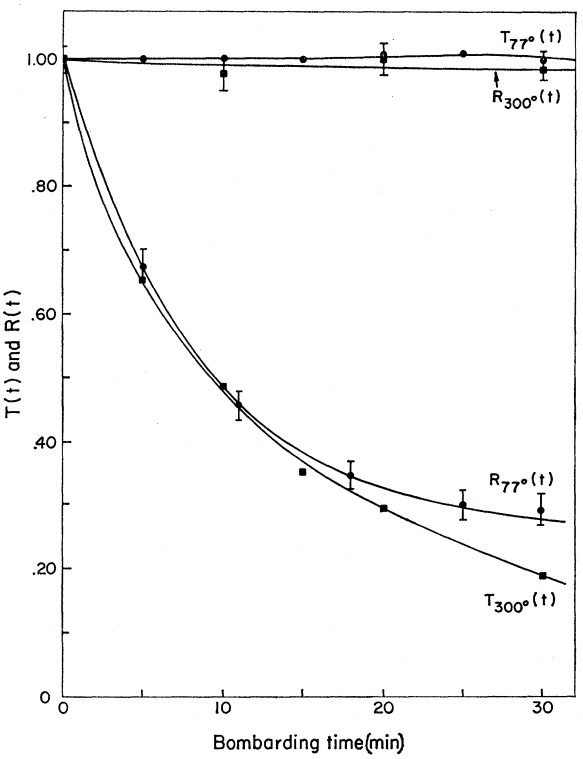

FIG. 5. The transmission coefficient $T(t)$ in the ⟨100⟩ direction normalized to zero time is shown as a function of time. $R(t)$ is the ratio of channeled intensity in the ⟨100⟩ direction to the intensity 7° off the channel axis in the (100) plane normalized to zero time. The figure 300° refers to measurements with the copper cylinder near the gold foil at room temperature and the figure 77° refers to measurements with the copper cylinder at liquid-nitrogen temperatures. Bombarding particles are 8-keV D^+ ions and the current density is on the order of 10^{-7} A/cm².

Time Dependence

The transmitted intensity i and the energy loss ΔE_{mp} are both found to be functions of time. The energy loss increases with time while the intensity normally decreases. The time dependence can easily be measured, however; the rate of change in the energy loss is small enough, so that no correction has to be considered here. The reason for the change in the transmitted intensity is studied to some extent by keeping the copper shield in the vicinity of the gold film at different temperatures. The function $T(t)$ is defined as the ratio of transmitted to incident ion current normalized to zero time. $R(t)$ is defined in the (100) plane as the channeled intensity $(i_{\theta=0°}-i_{\theta=7°})$ normalized to zero time. This ratio is expected to be sensitive to changes in the gold crystal. In Fig. 5 $T(t)$ and $R(t)$ are shown with the copper shield at room temperature (300°K) and at liquid-nitrogen temperature (77°K). With the copper shield at 77°K the contamination of the gold crystal is reduced and the functions $T(t)$ and $R(t)$ reflect the effects of true radiation damage. With the copper shield at 77°K the normally observed contamination spot was not visible on the gold film at the end of the 30-min bombardment.

Charge Exchange

The interpretation of our results are based on the assumption that for these low energies, charge exchange with the bombarded material is independent of orientation. If we assume that the reflection coefficient is very small, we find that for 30-keV He^+ ions, the fraction of the incident intensity which emerges from a 300-Å gold crystal as He^+ ions is about 0.2. This value is obtained by measuring the transmitted intensity as a function of α and integrating over all forward directions with a correction applied for the finite detector aperture. Neutral He atoms are not detectable with the arrangement used here. It is very likely that in our experiment the charge exchange takes place in the contamination layer which tentatively consists of elemental carbon. The figure 0.2 is then in reasonable agreement with an extrapolation of measurements at higher energies.[29]

Crystal Defects and Thermal Vibrations

Evaporated gold films are known to contain appreciable concentrations of defects. The peak intensities are believed to be affected by these defects and by thermal vibrations. In particular, when the channel area becomes small, the effect might be large enough to knock ions out of the channel direction.

A "cutoff" in the directional channeling has also been observed. The critical area for 23-keV D^+ ions is found to be close to the ⟨019⟩, ⟨1,1,10⟩, or ⟨167⟩ directions. If the root-mean-square (rms) amplitude of the thermal vibrations amounts to about $0.03a_0$ at 300°K and the radius of the D^+ ion is neglected compared to the gold atom, the critical channel area corresponds to a hard-sphere radius of $0.04a_0$.

DISCUSSION

Peak-Width Errors

There are several sources of error which might effect the widths of the peaks. We will give a brief discussion of each of these.

(*a*) *Detector angle.* A numerical estimate of the effect on the peakwidth of different detector openings has been made. It is found that if half of the acceptance angle of the detector, σ_{det}, is equal to $0.5_{2\theta}$, the measured width is 3% too large. If $\sigma_{\text{det}}=\sigma_{2\theta}$ the correction is 8%. In all runs $\sigma_{\text{det}}<0.3\sigma_{2\theta}$. A correction of 2% may be applied to $\sigma_{2\theta}$.

(*b*) *Beam spread.* From the diameter of the contamination spot and the beam defining aperture, half of the angular spread σ_{beam} is found to be 0.14°. We thus find that $\sigma_{\text{beam}}<0.1\sigma_{1\theta}$. No correction is necessary.

(*c*) *Wrinkles.* All foils have been examined in an optical microscope for wrinkles in the central area of the foil. Only foils with at least 4–9 perfectly flat grid squares in the center have been used. No wrinkles are seen after the bombardment. No correction is necessary. For some of the films, electron microscope photographs show bend extinction contours which indicate the presence of submicroscopic wrinkles. The effect of these is believed to be small.

(*d*) *Grid-Square Misorientation.* Microscope grids looking perfectly flat to the naked eye have been checked in the optical microscope. It is found that individual grid squares can be tilted a small angle relative to their neighbors. A maximum tilt of about 1° is observed. The standard deviation σ_{grid} is equal to about 0.5°. We find that $\sigma_{\text{grid}}<0.3\sigma_{2\theta}$. A correction of 2% may be applied to $\sigma_{2\theta}$.

(*e*) *Angular Measurements.* The accuracy in setting the dials for θ and α is about 0.25°. A gear ratio of 2:1 in the dial for φ makes it possible to set φ within 0.15°. The statistical errors in measuring σ_θ, σ_φ, and $\sigma_{2\theta}$ are therefore 0.1°–0.2°. No goniometer play has been observed. We find $\sigma_{\text{gear}}\ll\sigma_{2\theta}$. No correction is necessary.

(*f*) *Surface Contamination.* The effect of surface contamination is very obvious from the study of the variation of peak intensities with time (Fig. 5). It is assumed that the contamination layer consists of elemental carbon.[30] From a comparison between the mean-square deflection angles for a 850-Å polycrystalline gold film and a 100-Å carbon film[31] we find that the additional spread in the incident ion beam due to a 100-Å carbon film is about 0.13°. The effective beam spread σ_{beam} is still only $0.15\sigma_{2\theta}$. A correction of 1% may be applied to $\sigma_{2\theta}$ because of the spread in the bombarding ion beam.

Because of (*a*), (*b*), (*d*), and (*f*), the measured values are about 3–5% too high. The statistical errors are about 5–10%.

Errors in Energy Determination

When only a single energy value, corresponding to maximum intensity in a specific direction, is measured the accuracy is ±2% for high intensities and 5–7% for low intensities. When the complete energy profile is determined the accuracy in locating the most probable energy of a particular beam component is about ±1.5%.

The rate of change of ΔE_{mp} as a function of time is found to be approximately 20% during the first hour of bombardment. This change in energy loss affects mainly the ungoverned motion. The heights of the peaks above the random energy loss in the energy-loss curves are less dependent on time. No corrections have been applied to any energy values presented in the figures or the tables.

Errors in Intensity Measurements

The experimental error in measuring the transmitted intensity for an individual point is less than 1% for

[29] J. C. Armstrong, J. V. Mullendore, W. R. Harris, and P. Marion, Proc. Phys. Soc. (London) 86, 1283 (1965).

[30] A. E. Ennos, Brit. J. Appl. Phys. 4, 101 (1953).

[31] N. F. Mott and H. S. W. Massey, *The Theory of Atomic Collisions* (Clarendon Press, Oxford, England, 1949), 2nd ed.

high intensities and about 5% for low intensities. The relative error in separating the directional from the planar channeling is about 10%. The error in the transmission coefficient $T(l)$ in Fig. 5 is about 5%.

Analysis of Peak Widths

We now try to find relationships between measured values of σ_θ, σ_φ, $\sigma_{1\theta}$, and $\sigma_{2\theta}$. Assume that the Gaussian distributions on the entrance side $P_{1\theta}$ and exit side $P_{2\theta}$ are independent and symmetric around the channel axis. Assume further that $\sigma_{1\theta}\neq\sigma_{2\theta}$. Then the relationship between $P_{1\theta}$, $P_{2\theta}$, and P_θ should be

$$P_\theta = P_{1\theta}\cdot P_{2\theta}, \tag{5}$$

which gives the relation

$$\sigma_\theta^{-2} = \sigma_{1\theta}^{-2} + \sigma_{2\theta}^{-2}. \tag{6}$$

The measured quantities given earlier do satisfy this relation. It is found that usually $\sigma_{2\theta}$ is larger than $\sigma_{1\theta}$. The critical angle for channeling[16] is expected to increase as the energy decreases. Since the energy decreases as the ion traverses the foil, the larger value of $\sigma_{2\theta}$ may be due to the increased critical angle for the ions emerging from the foil.

When the ions are detected at a fixed angle $\alpha_0\neq 0$, it is found that the peaks in the transmitted intensity measured as a function of θ are shifted. Assuming that $\sigma_{1\theta}=\sigma_{2\theta}$ it is obvious that $P_\theta=\exp\{-[(\theta-\theta_0)^2/2\sigma_{1\theta}^2] - (\theta-\theta_0-\alpha_0)^2/2\sigma_{2\theta}^2\}$ has a maximun for a shift $\delta\theta$ given by

$$\alpha_0/\delta\theta = 2. \tag{7}$$

Table II gives the measured ratios $\alpha_0/\delta\theta$ for three values of α_0 using 9-keV D^+ ions in a 660 Å±40 Å gold film. It shows that in this particular experiment the assumption that $\sigma_{1\theta}=\sigma_{2\theta}$ leading to (7) is not the best assumption. If instead $\sigma_{1\theta}$ is assumed to be $0.8\sigma_{2\theta}$, it can be shown by maximizing P_θ that the calculated ratio $\alpha_0/\delta\theta$ agrees with the average measured value of 2.6 in Table II. The directly measured values of $\sigma_{1\theta}$ and $\sigma_{2\theta}$ given above give a ratio of 0.74.

If φ is changed across a channel peak with $\alpha=0$ and $\theta=\theta_0$, we effectively change the angle β between the channel axis and the beam direction. The relationship between β and a change $\Delta\varphi=\varphi-\varphi_0$ for small values of β and $\Delta\varphi$ around the channel axis can be shown to be

$$\beta/\Delta\varphi = \sin\theta. \tag{8}$$

If the channel peak has rotational symmetry, the characteristic widths σ_θ and σ_φ should be related by the equation

$$\sigma_\theta/\sigma_\varphi = \sin\theta. \tag{9}$$

Figure 6 shows the experimental ratios of $\sigma_\theta/\sigma_\varphi$ for four channel peaks in the (100) plane. The solid curve is the function $\sin\theta$. Six different foils are used. The agreement is very good and proves that the difference between

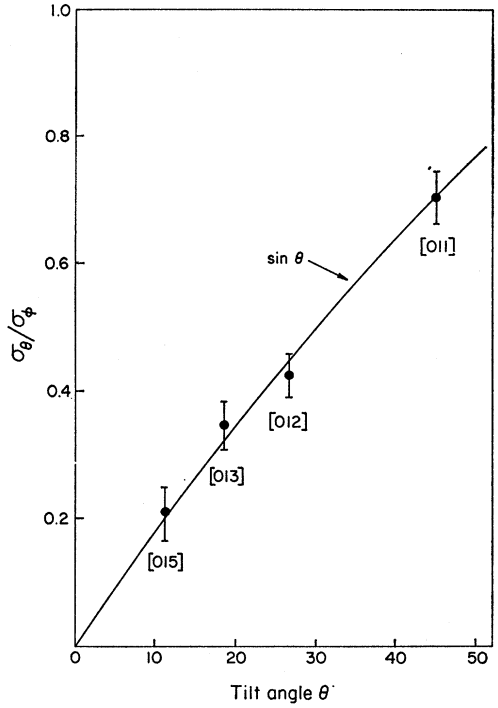

FIG. 6. A comparison between $\sin\theta$ (solid line) and $\sigma_\theta/\sigma_\varphi$ (filled circles) for four channels in the (100) plane; six different gold foils are used. The agreement between $\sigma_\theta/\sigma_\varphi$ and $\sin\theta$ shows that the peaks are summetric around the channel axis.

σ_θ and σ_φ is not characteristic of the crystal, but originates from geometrical factors in the goniometer. The peaks are thus quite symmetric around the channel axis.

Analysis of Energy Losses

The total energy loss is the sum of nuclear and electronic losses. To compare the measured dE/dx values with theory we have used the expression by Nielsen[24] for the energy loss due to displacement collisions:

$$\frac{dE^{(N)}}{dx} = 3.63\frac{NM_1}{M_1+M_2}\frac{Z_1Z_2e^2}{(Z_1^{2/3}+Z_2^{2/3})^{1/2}}\frac{\hbar^2}{m_e e^2}. \tag{10}$$

For the electronic loss we use the expression by Lindhard and Scharff[25]:

$$\frac{dE^{(LS)}}{dx} = \frac{N8\pi e^2 a_0 Z_1 Z_2}{(Z_1^{2/3}+Z_2^{2/3})^{3/2}}\frac{v}{v_0}\xi_\epsilon. \tag{11}$$

In (10) and (11), N stands for the number of nuclei per unit volume. The indices 1 and 2 denote the bombarding and the target particle. a_0 is the Bohr radius and ξ_ϵ is a parameter of the order of unity. v_0 is equal to $e^2/\hbar$. In (10) the ratio b/a between the impact parameter b and the screening radius a is limited to the interval 0.8

$<(b/a)<15$. The ratio $K=b/\lambda$ must be large compared to unity where λ is the de Broglie wavelength of the incident particle.

According to Dienes and Vineyard,[32] the electronic loss (11) to the conduction electrons is important when the energy

$$E>M_1\epsilon_F/16m_e, \tag{12}$$

where ϵ_F is the Fermi energy for gold (5.6 eV). The critical energy for He^+ ions in gold is, according to (12), about 3 keV. Tables III and IV list the calculated and measured quantities for 25-keV He^+ ions traveling through the 275-Å single-crystal gold film in Fig. 2 and for 23-keV and 13-keV D^+ ions transmitted through the 550-Å gold film in Fig. 3. Because of the fairly large energy loss in the foils the average velocity $\bar{v}$ over the region in which dE/dx is measured is used instead of v. In Table IV the last column lists the percentage decrease, $(\Delta E_{mp}{}^r-\Delta E_{mp})/\Delta E_{mp}{}^r$, in the energy loss for He^+ and D^+ ions channeled through three of the most open channels in a fcc lattice. $\Delta E_{mp}{}^r$ denotes the most probable energy loss of the random part of the beam.

In the ⟨112⟩ direction $(\Delta E_{mp}{}^r-\Delta E_{mp})/\Delta E_{mp}{}^r$ is found to be about 11% for He^+ ions in gold. Almost the same figure is obtained if the energy loss is measured in the (111) plane at a φ value off the [112] direction and corresponding to a high-index plane of the type $(hk0)$. This fact indicates that the percentage reduction in the (111) plane is also about 11%. At $\theta=0$ only (100) planes contribute to the channeling. The percentage reduction in energy loss due to this type of plane is found to be about 7%. The (110) plane does not show up at all. The order of importance amongst the planes is thus found to be (111), (100), and (110) which is the same order as was found above.

The energy loss has also been measured in the ⟨001⟩ direction as a function of foil thickness. In the thickness range 275 Å to 1000 Å, the function is very linear. The slope of the line gives a value 7.4±0.3 eV/Å for the stopping power (dE/dx) in the ⟨001⟩ direction.

[32] G. J. Dienes and G. H. Vineyard, *Radiation Effects in Solids* (Interscience Publishers, Inc., New York, 1957).

CONCLUSIONS

(1) The transmitted intensity of D^+ and He^+ ions of 8–25 keV energy through thin single-crystal gold films (275–600 Å) consists of directional and planar contributions as well as of a randomly scattered part. (2) The order amongst the three most open directions is found to be ⟨011⟩, ⟨001⟩, and ⟨112⟩. (3) Intensity as well as energy loss measurements give the order (111), (100), and (110) amongst the three most important planes. (4) A "cutoff" in the planar channeling exists between the planes (100) and (110). (5) The peaks are symmetrical around the channel axes and the over-all peak widths are successfully interpreted in terms of the channel entrance and exit peak widths. (6) Energy-loss measurements in high-index directions agree satisfactorily with theoretical predictions for the stopping power dE/dx. (7) The difference in energy loss between directional and planar channeling is much less pronunced than the difference in the channeled intensity showing that the effect of channeling on the energy loss is a secondary effect. (8) Charge exchange is found to significantly reduce the fraction of the beam which emerges from the foil as ions. (9) From the observed cutoff in the directional channeling at high indices, the effective hard-sphere radius for 23-keV D^+ ions in gold is estimated to be 0.16 Å.

ACKNOWLEDGMENTS

The authors would like to express their sincere gratitude to Dr. E. F. Wassermann for critically reading the manuscript. We would also like to thank W. Morris for many helpful discussions, D. Weber for operating the electron microscope, and W. Krakow for making the gold films.